

Suppression of Superfluidity upon Overflow of Trapped Fermions. Quantal and Thomas-Fermi Studies

P. Schuck^{1,2}, X. Viñas³

¹Institut de Physique Nucléaire,
IN2P3-CNRS, Université Paris-Sud,
F-91406 Orsay-Cédex, France

²Laboratoire de Physique et Modélisation des Milieux Condensés,
CNRS and Université Joseph Fourier,
25 Avenue des Martyrs, Boîte Postale 166,
F-38042 Grenoble Cedex 9, France

³Departament d'Estructura i Constituents de la Matèria and Institut de Ciències del Cosmos,
Facultat de Física, Universitat de Barcelona,
Diagonal 647, E-08028 Barcelona, Spain

Two issues are treated in this work: (i) the generic fact that if a fermionic superfluid in the BCS regime overflows from a narrow container into a much wider one, pairing is much suppressed at the overflow point. Physical examples where this feature may play an important role are discussed. (ii) A Thomas-Fermi (TF) approach to inhomogeneous superfluid Fermi-systems is presented and shown that it works well in cases where the Local Density Approximation (LDA) breaks down.

Superfluid fermions in finite systems can exist in traps of cold atoms, in nuclear systems, in small metallic clusters, etc. An interesting question arises what happens to the superfluid if its Fermi level reaches the edge of a finite container, i.e. either the fluid overflows into the continuum or it pours into another container of much larger dimension. A trapping potential of this type has experimentally already been generated for the study of cold bosonic atoms [1]. It should also be possible to use it for fermionic atoms [2].

In the inner crust of neutron stars, there also may occur the situation where coexists a superfluid neutron gas of variable density in between the lattice of (superfluid) nuclei [3, 4]. This situation often is mimicked by a Wigner Seitz cell, where the single particle potential has a pocket, representing the nucleus, embedded in a large container. Still other systems may exist with similar situations.

The purpose of this work is to study superfluidity of fermions at the overflow (drip) in the BCS regime. Since the quantal solution of BCS equations in geometries with rapidly varying single particle potentials with a large number of particles is numerically difficult, we will present, as a second objective of this work, a Thomas-Fermi approach to inhomogeneous superfluidity which shows good performance in situations where LDA fails.

For our study we first will use a schematic model of slab geometry with a transverse potential of large extension L possessing at the origin a 'pocket' of variable depth and size R much smaller than the outer container. Schematically such a potential is shown in Fig. 1a. This slab configuration may roughly mock up one sheet of a so-called Lasagne configuration in the inner crust of neutron stars [5]. We, therefore, will use nuclear dimensions for the slab model but they can easily be replaced by dimensions relevant for other systems. Our model and the ensuing generalisations treated below, therefore, are believed to be generic. We will study the slab configuration also because the quantal solution of the gap equation is evaluated relatively directly and the quality of the TF approach can thus be established. Once this is achieved, we also will go over to other geometrical configurations. We, for instance, will treat a second potential shown in Fig. 1b with spherical symmetry, a kind of which, as already mentioned, has been used for bosonic atoms in [1].

The wave functions and eigenenergies of a box as shown in Fig. 1a with a potential-hole are given in [6]. For pairing, we use a contact force with a cut off Λ , to make things simple. Integrating over momenta in slab direction the usual gap equation $\Delta_n = \sum_{n'} \int \frac{d^2p}{(2\pi\hbar)^2} V_{nn'} \Theta(\Lambda - \varepsilon_{n'} - \varepsilon_p) \Delta_{n'} / (2E_{n'}(p))$ with $E_n(p) = \sqrt{(\varepsilon_n + \varepsilon_p - \mu)^2 + \Delta_n^2}$ the quasiparticle energy, $\Theta(x)$ the step function, and $\varepsilon_n, \varepsilon_p$ being the discrete single particle energies in trans-

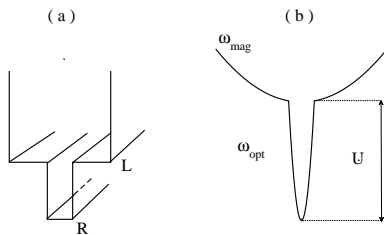


FIG. 1: Schematic view of the potentials used in this work. Panel (a) shows a perspective view of the slab potential which is translationally invariant in x, y direction. Panel (b) represents a spherically symmetric container

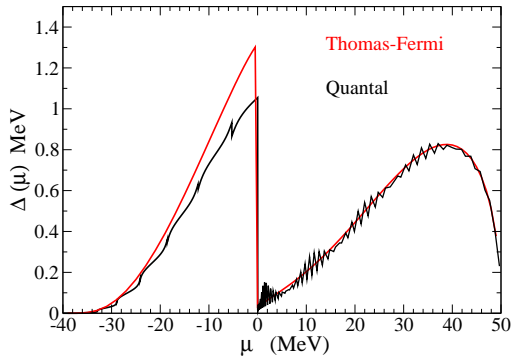


FIG. 2: (Coloronline) Quantal and TF pairing gap in the slab geometry as a function of the chemical potential.

verse direction and kinetic energies in slab direction, respectively, one arrives at the following gap equation

$$\Delta_n = - \sum_{n'} \Theta(\Lambda - \varepsilon_{n'}) V_{nn'} K_{n'} \quad (1)$$

with

$$K_n = \frac{m}{4\pi\hbar^2} \Delta_n \ln \frac{\Lambda - \mu + \sqrt{(\Lambda - \mu)^2 + \Delta_n^2}}{\varepsilon_n - \mu + \sqrt{(\varepsilon_n - \mu)^2 + \Delta_n^2}} \quad (2)$$

where m is the particle mass and the indices n stand for the level quantum numbers in the confining potential of Fig. 1a. The matrix elements $V_{nn'} = -g \int_{-L}^{+L} |\varphi_n(z)|^2 |\varphi_{n'}(z)|^2 dz$ of the contact force $-g\delta(\mathbf{r} - \mathbf{r}')$ can be evaluated straightforwardly from the wave functions $\varphi_n(z)$ given in [6].

For an example we take as cut off $\Lambda = 50$ MeV counted from the edge of the pocket potential whose depth be $V_0 = -40$ MeV. Its extension ranges from $-R$ to $+R$ with $R = 10$ fm. The wide potential with infinite walls has extension from $-L$ to $+L$ with $L = 100$ fm. For the coupling strength we take $g = 150$ MeV fm³.

Before we show the results, let us explain our Thomas-Fermi (TF) approach for this problem. For this, we transform Eq.(1) into a continuum version in the following way. We first consider the Wigner transform of the density matrix corresponding to the state $|n\rangle$: $[\hat{\rho}_n]_W = [|n\rangle\langle n|]_W$ and take the $\hbar \rightarrow 0$ limit of this expression, see [7–9]

$$f_E(z, p) = \frac{1}{g^{TF}(E)} \delta(E - H_{cl.}) + O(\hbar^2) \quad (3)$$

where $H_{cl.} = \frac{p^2}{2m} + V(z)$ is the classical Hamiltonian with $V(z)$ the potential (Fig. 1a) in transverse direction and

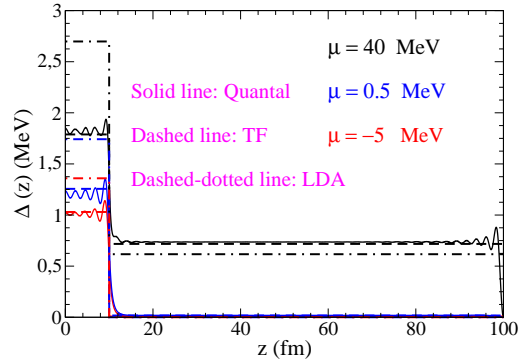


FIG. 3: (Coloronline) Position dependence of the gap in the slab geometry for different values of the chemical potential. Quantal, TF, and LDA results are shown. Notice that Δ for $\mu = 0.5$ and -5.0 MeV is practically zero in the gas region.

$g^{TF}(E)$ is the corresponding level density to lowest order in \hbar , i.e. the usual TF expression [9]. Quantum numbers and energies are simply characterised by the continuous energy variable E which takes the place of the discrete values ε_n in the quantal case.

The TF version of the gap equation (1) then reads

$$\Delta(E) = - \int_{V_0}^{\Lambda} dE' g(E') V(E, E') K(E') \quad (4)$$

with $K(E)$ an obvious generalisation of K_n . The matrix elements $V(E, E')$ can be evaluated in replacing $|\varphi_n(z)|^2$ by [7] $\rho_E^{TF}(z) = \frac{1}{g^{TF}(E)} \frac{1}{2\pi} \left(\frac{2m}{\hbar^2}\right)^{1/2} [E - V(z)]^{-1/2}$, the on-shell TF density in transverse direction. As the reader will easily realise, the way of proceeding is very different from usual LDA where the finite size dependence is put into the (local) chemical potential whereas here it is put into the matrix elements of the pairing force.

We are now in a position to solve the quantal and TF gap equations for the above mentioned parameter values of our model. The result for the gap at the chemical potential μ is shown in Fig. 2 as a function of μ . We start with μ from the bottom of the pocket well, i.e. with zero density. We then increase μ , i.e. the density. We see that once the fill up of the pocket reaches its top, the values of the gap sharply drop and practically reach zero. In the continuum the gaps slowly rise again. We see that quantal and TF values are in close agreement. The overshoot of the TF solution for negative μ very likely is due to the smallness of the pocket which only can accommodate nine bound levels. It may be partially cured including \hbar corrections [9] which, however, we do not consider here. Before we come to an explanation of the drop of the gaps at overflow (drip), let us study the gaps as a function of position in transverse direction: $\Delta(z) = -gK(z)$ with

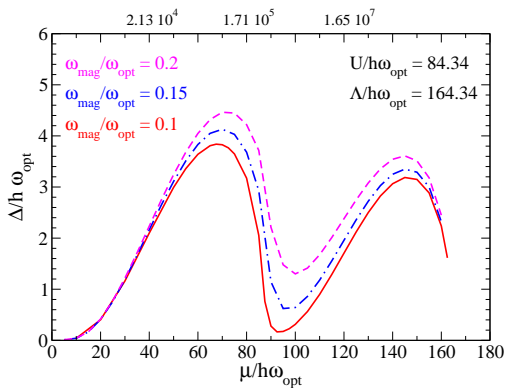


FIG. 4: (Coloronline) Average TF gaps at the Fermi energy as a function of the chemical potential for the potential shown in Fig. 1b. In the completely filled optical trap ($\mu = U$) we accommodate 10^5 atoms in each spin state. The total number of atoms in the trap with $\mu/\hbar\omega_{opt}=40, 80$ and 120 are indicated in the upper horizontal axis.

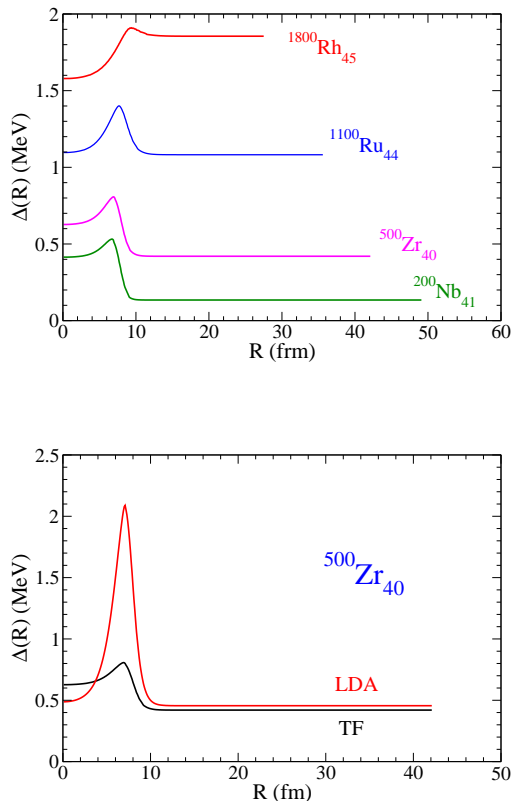


FIG. 5: (Coloronline) Upper panel: Radial dependence of the TF gap in the considered WS cells. The end points indicate the radius of the WS cells. Lower panel: Comparison between TF and LDA gaps as a function of the position in a WS cell containing a single ${}^{500}_{40}\text{Zr}$ nucleus.

$K(z) = \sum K_n |\varphi_n(z)|^2$. Semiclassically, this expression becomes: $K(z) = \int_{V_0}^{\Lambda} dE g^{TF}(E) K(E) \rho_E^{TF}(z)$.

In Fig. 3, we show the density profiles for three values of μ : $\mu = 40, 0.5$, and -5 MeV. We see that quantal and TF results agree, up to shell fluctuations, very well. We also show the LDA results. We see that they can be as wrong as by 50 percent. For other choices of system parameters the LDA error may even be worse. This stems from the fact that in TF (and, of course, also quantally), there is coupling between inside and outside the pocket, i.e. the Cooper pair wave function extends into both regions what tends to equilibrate the values of the gaps. In LDA the contrast is much too strong. The drop of the gaps when crossing the threshold can be explained by the fact that the single particle states are strongly delocalised in the outer container and, thus, their contribution to the pairing matrix element $V_{n,n'}$ becomes very small.

Having gained faith into our TF approach, we now can explore other geometries and other systems, more difficult for quantal solutions. In Fig. 4 we show the result for Δ in the spherical double harmonic oscillator potential shown in Fig. 1b which may be realised with cold fermionic atoms to study the overflow situation. A zero range force with strength $g=-1.0$ and cut off $\Lambda=164.34$ (in the corresponding optical trap units with $\omega_{opt} = 2\pi \times 1000$ Hz taken from [2]) is used. We see that the result is qualitatively similar to the slab case though in this spherical geometry the dip does not quite reach zero and also is shifted slightly to an energy above the break of the potential. Note that this depends strongly on the choice of the ratio $\omega_{mag}/\omega_{opt}$ as it can be seen in the figure. Also the gap starts to decrease towards the minimum quite early. It shall be interesting to see whether our prediction can be verified experimentally.

Let us now make a more realistic study of Wigner-Seitz (WS) cells including electrons in β equilibrium to simulate the inner crust of neutron stars [5]. To this end the mean-field is computed selfconsistently using the BCP energy density functional [10] together with the TF approach as explained in [11]. The semiclassical description of the WS cells including pairing correlations at TF level is obtained from this mean-field using the finite range part of the Gogny D1S force [12] in the pairing channel [13]. It must be pointed out that the total energy per baryon obtained with our TF approach is in very good agreement with the old quantal calculation of Negele and Vautherin [14] as it is explicitly discussed in Ref.[11]. In Fig. 5 are displayed the corresponding gaps with their radius dependences. It is seen that when the gap is small outside the region of the nucleus, then the gap also is small inside the nucleus. This stems from the very large coherence length where one neutron of a Cooper pair can be in the huge volume of the gas and the other inside the small volume of the nucleus (proximity effect). In this way the gas imprints its behavior for the gap also inside the nucleus. Such a conclusion was also given in a quantal

Hartree-Fock-Bogoliubov (HFB) calculation by Grasso et al. in [15] what shows that the here employed BCS approximation apparently yields very similar answers as a full HFB calculation for WS cells [3, 16]. Finally, in the lower panel of Fig. 5 we show a comparison of LDA and present TF results for a particular WS cell. We see a huge difference in the surface region of the nucleus. This simply stems from the fact that in this case of the $^{500}_{40}\text{Zr}$ nucleus in the WS cell the gap is very small and, therefore, the coherence length very large invalidating LDA. A study with examples a little less unfavorable for LDA is given in [17].

For isolated nuclei at the neutron drip the situation may be different. It seems that in this situation the difference between HFB and BCS approaches may be significant. Somewhat conflicting results in this respect exist in the literature. In ref [18] very similar results to ours are found for S-wave pairing. On the other hand in [19] the gap seems to rise towards the drip before it bends down. Similar results have recently been found in [20]. Preliminary investigations show that these discrepancies may be due to large shell fluctuations in isolated nuclei. More studies in this direction seem to be necessary.

Summarizing, we have studied superfluid fermions in a large container, either external (cold atoms) or created self consistently (nuclei) for situations where the top of the fluid reaches the edge of a small pocket situated at the origin of the wide confining potential. The gap drops to zero at the edge before rising again when the density fills up the outer container. This at first somewhat surprising phenomenon can be explained quite straightforwardly. Such situations, as already mentioned, can exist in cold atoms and nuclei in the inner crust of neutron stars, two examples treated here with their specific form of containers. For small systems like isolated nuclei at the neutron drip, the situation may be blurred by shell effects.

As an important second aspect of this work, we showed that a novel Thomas-Fermi approach to inhomogeneous situations can cope with situations where LDA fails. This means that our TF approach is free of the restrictive condition, prevailing for LDA, that the Cooper pair coherence length must be shorter than a typical length l (the oscillator length in the case of a harmonic container) over which the mean field varies appreciably. On the contrary, our TF theory has the usual TF validity criterion, namely that local wavelengths must be shorter than l .

The accuracy of our TF approach opens wide perspectives for a treatment of inhomogeneous superfluid Fermi-systems with a great number of particles not accessible for a quantal solution of the BCS (HFB) equations. Such systems may be cold atoms in deformed containers (eventually reaching millions of particles), superfluid-normal fluid (SN) interfaces, vortex profiles, etc. As a matter of fact, as is well known [9], the TF approach becomes the more accurate, the larger the system. Thus the TF ap-

proximation is complementary to the quantal one in the sense that the former works where the latter is difficult or even impossible to be obtained numerically.

We thank W. Ketterle and A. Minguzzi for their interest in this work and for pointing out refs. [1, 2]. We are grateful to Michel Farine for contributions and to Michael Urban for useful discussions and a critical reading of the manuscript. We also thank K. Hagino for pointing to Ref.[19] and sending their own results prior to publication. This work has been partially supported by the IN2P3-CAICYT collaboration (ACI-10-000592). One of us (X.V.) acknowledges grants FIS2008-01661 (Spain and FEDER), 2009SGR-1289 (Spain) and Consolider Ingenio Programme CSD2007-00042 for financial support.

-
- [1] D.M. Stamper-Kurn, H.-J. Miesner, A.P. Chikkatur, S. Inouye, J. Stenger and W. Ketterle, Phys. Rev. Lett. **81**, 2194 (1998).
 - [2] L. Viverit, S. Giorgini, L.P. Pitaevskii and S. Stringari, Phys. Rev. **A63**, 033603 (2001).
 - [3] M. Baldo, U. Lombardo, E.E. Saperstein and S.V. Tolokonnikov, Nucl. Phys. **A750**, 409 (2005); M. Baldo, E.E. Saperstein and S.V. Tolokonnikov, Eur. Phys. J. **A32**, 97 (2007).
 - [4] N. Chamel, S. Goriely, J.M. Pearson and M. Onsi, Phys. Rev. **C81**, 045804 (2010).
 - [5] P. Haensel, *Neutron Stars 1: Equation of State and Structure*, (Springer-Verlag, New York, 2007).
 - [6] S. Flügge, *Practical Quantum Mechanics*, (Springer-Verlag, Berlin, 1974).
 - [7] X. Viñas, P. Schuck, M. Farine and M. Centelles, Phys. Rev. **C67**, 054307 (2003).
 - [8] X. Viñas, P. Schuck and M. Farine, Int. J. Mod. Phys. **E20** 399 (2011)
 - [9] P. Ring and P. Schuck, *The Nuclear Many-Body Problem*, (Springer-Verlag, Berlin, 1980).
 - [10] M. Baldo, P. Schuck and X. Viñas Phys. Lett. **B663**, 390 (2008).
 - [11] X. Viñas, P. Schuck and M. Farine, arXiv:1106.0187, J. of Phys.:Conf.Ser. **321**. 012024 (2011).
 - [12] J. Dechargé and D. Gogny, Phys. Rev. **C21**, 1568 (1980); J.-F. Berger, M. Girod and D. Gogny, Comp. Phys. Comm. **63**, 365 (1991).
 - [13] The D1S force for pairing has been multiplied with a factor 0.85 to compensate for the use of the bare mass in the calculation.
 - [14] J.W. Negele and D. Vautherin, Nucl. Phys. **207**, 298 (1973).
 - [15] M. Grasso, E. Khan, J. Margueron and N. Van Giai, Nucl. Phys. **A807**, 1 (2008).
 - [16] Our TF theory can be generalised to the HFB case what shall be done in future work.
 - [17] A. Pastore, F. Barranco, R.A. Broglia, and E. Vigezzi, Phys. Rev. **C78**, 024315 (2008).
 - [18] I. Hamamoto, Phys. Rev. **C71**, 037302 (2005).
 - [19] N. Tajima, Eur. Phys. J. **25**, 571 (2005).
 - [20] K. Hagino and H. Sagawa, arXiv:1105.5469